IOP Conference Series: Materials Science and Engineering

PAPER • **OPEN ACCESS**

Improved Positioning of Delivery Quad copter Using GPS - Accelerometer Multimode Controller and Unscented Kalman Filter

To cite this article: Ahmed Abdulmahdi Abdulkareem Alawsi *et al* 2020 *IOP Conf. Ser.: Mater. Sci. Eng.* **745** 012018

View the article online for updates and enhancements.

This content was downloaded from IP address 151.236.176.243 on 12/08/2020 at 20:29

IOP Conf. Series: Materials Science and Engineering **745** (2020) 012018 doi:10.1088/1757-899X/745/1/012018

Improved Positioning of Delivery Quad copter Using GPS - Accelerometer Multimode Controller and Unscented Kalman Filter

Ahmed Abdulmahdi Abdulkareem Alawsi[1], **Basil H Jasim**[2] and **Safanah Mudheher Raafat**[3]
[1]College of Science, Physics Dept., University of Wasit, Wasit, Iraq
[2]Electrical Engineering Dept., University of Basra, Basra, Iraq
[3]Control and System Engineering Dept., University of Technology, Baghdad, Iraq
Correspondence: hanbas632@gmail.com

Abstract: In last area of technology, the quadrotor helicopter became essential equipment of everyday man use. Delivery by quadcopter has increased significantly in the last few years in different private and military fields because of its indispensable features such as autonomous flight, vertical take-off and landing. Most quadcopters used for delivery service utilize GPS signal for its autonomous flight to control itself and follow the desired path to the destination. Despite the prevalence of autonomous flight, it produces many challenges. GPS signal denial is one of the most critical challenges that may occur. GPS signal denial problem leads to affect the quadcopter control and potentially get lost. Many studies have tried to provide a solution toward this issue, yet, most solutions focused on specific applications and terms rather than achieving a general solution. In this paper, a multimode control algorithm is proposed as a solution for GPS signal denied through the autonomous flight. The algorithm consists of two control modes: GPS and accelerometer modes with Unscented Kalman Filter (UKF). The results show that the proposed algorithm is reliable and suitable for various applications of the quadcopter in different environments. The proposed algorithm can keep the quadcopter under control during GPS signal denial period and continue moving toward the desired path.

Keywords Quadcopter, PID, controller, autonomous flight, delivery by quadcopter, GPS signal interruption, UKF

1. Introduction

In the last decade, applications of quadcopters have been exponentially increased as a result of their low-cost production, the capability of vertical take-off and landing within a small area, and also their ability to implement complex tasks [1].

In the past, a quadcopter was mainly used for military applications. However, lightweight, mechanical structure as well as properties mentioned above have led to application expansion to areas such as delivery, emergency search and rescue, traffic control, cargo transport, weather monitoring, forest fire detection, agricultural usage, communication relaying, medical usage, building and bridge cracked monitoring [1, 2]. In particular, delivery by the quadcopter is increasingly being considered as a means to overcome ground traffic problems [3].

Autonomous flight is the standard technique of quadcopter delivery applications. Quadcopter uses a GPS signal to follow a desired trajectory towards a destination [3-5]. For the quadcopter to remain under control, the controller must continuously receive a linear position measured by the GPS sensor as well as angular position measured by the gyroscope sensor. However, problems arise when the GPS signal is inevitably disrupted by environmental stimuli, such as navigation between high buildings, under a bridge, above a power station, etc. [5]. Consequently, the quadcopter is going out of control, and this restricts the fundamental functionality of quadcopters.

Multiple algorithms and techniques have been proposed to solve the problem of GPS signal denial for special situations only. So, there has not been a successful approach that can be generalizable to quadcopter delivery applications more broadly. The main progress in previous attempts can be summarized as follows.

Content from this work may be used under the terms of the Creative Commons Attribution 3.0 licence. Any further distribution of this work must maintain attribution to the author(s) and the title of the work, journal citation and DOI.
Published under licence by IOP Publishing Ltd

Ononiwu *et al.* [2]: In this approach, the ground control station is used to control the quadcopter wirelessly via radio frequency. Gyroscope and Accelerometer sensors are used to measure current states of the quadcopter, while desired motor signals are measured through erroneous signals, as measured by the Proportional, Integral, and Derivative (PID) controller. This technique consumes great energy because it uses complex measurement algorithms caused by merging multiple measurement algorithms. Greater power consumption means a shorter battery time, which reduces the distance that the quadcopter can reach. In addition, radio signal interruptions through autonomous flight can occur due to environmental constraints; a problem that has not been argued.
Haque *et al.* [4]: In this approach, GPS signal is used to follow the desired path acquired from Google Maps over cellular networks. This method does not elaborate on the problem of GPS signal denial during flight. Also, this method consumes great energy because it uses different network devices. So, this method is not reliable to use for delivery by quadcopter.
Tada *et al.* [5]: This approach uses a simple method to address GPS signal denial and control the quadcopter under unstable GPS signal situations. The method consists of two searchlight sources on the ground, which can investigate target positions across a span of 50m. This method is novel and functional, but it designed to work with short distance so it can never be used to quadcopter delivery applications.
Hochstenbach *et al.* [6]: This approach involved a special Unmanned Arial Vehicle (UAV) quadcopter called hybrid VertiKUL which had two fixed wings and four rotors to implement the parcel delivery by air. It used GPS signal for fully autonomous parcel delivery but, like the method outlined in Haque *et al.* [4], this technique does not address the problem of GPS signal interruptions during flight. So, this method dose not reliable to use it for delivery by quadcopter.

In this paper, we propose a general solution for GPS signal denial via a new, multimode control algorithm to give for quadcopter to operate in different applications environment. The premise for the algorithm is as follows: the quadcopters in autonomous flight can be controlled by both GPS signals, and accelerometer signals, both of which have errors in measurement [7]. Errors in the measured state arise from uncertainty of mathematical calculation and physical sensors. Here, we demonstrate how to decrease those errors: The Unscented Kalman Filter (UKF) was used as a state estimator, and then added to (combined with) the dynamic model. PID controller was applied to the mathematical model to control the attitude and position of the quadcopter. All control modes (GPS mode only, GPS mode with denied signal, GPS mode + Accelerometer mode) are simulated with and without UKF by Matlab/simulink version 2018a. The results show that the proposed control algorithm is reliable and can keep the quadcopter under control through GPS signal denied period with simple fluctuations. Also, the UKF is used to increase the robustness of quadcopter control system by decreasing the fluctuations generated by physical sensors.
The rest of paper is organized as follows: Section 2 describes the mathematical model of the quadcopter, Section 3 gives a detailed description of proposed control method, Section 4 describes altitude and attitude controls by modified PID controller, Section 5 shows how to estimate the actual states by UKF, Section 6 gives a description of simulation block diagrams, Section 7 gives the results and discussion, and the conclusion is given in section 8.

2. Mathematical Model

In this section, the mathematical dynamic model of the quadcopter is derived and can be used to study the performance of the quadcopter by using suitable simulation programs. A quadcopter has four independently controllable actuators (motors) assembled in cross configuration, as shown in Figure 1. One pair of opposite motors rotate in the same direction (clockwise), while the other two motors rotate counter clockwise, so the affected rotational torque on the body around Z axis of the quadcopter is cancelled during hovering state [8].
Figure 1 shows two basic coordinate frames, called an inertial frame (fixed earth frame(E)) and a body frame (B). These two frames are used to identify the quadcopter's location and attitude, and then

translation and rotation matrices can be applied in order to transfer data from one coordinate frame to another [1, 8-10].

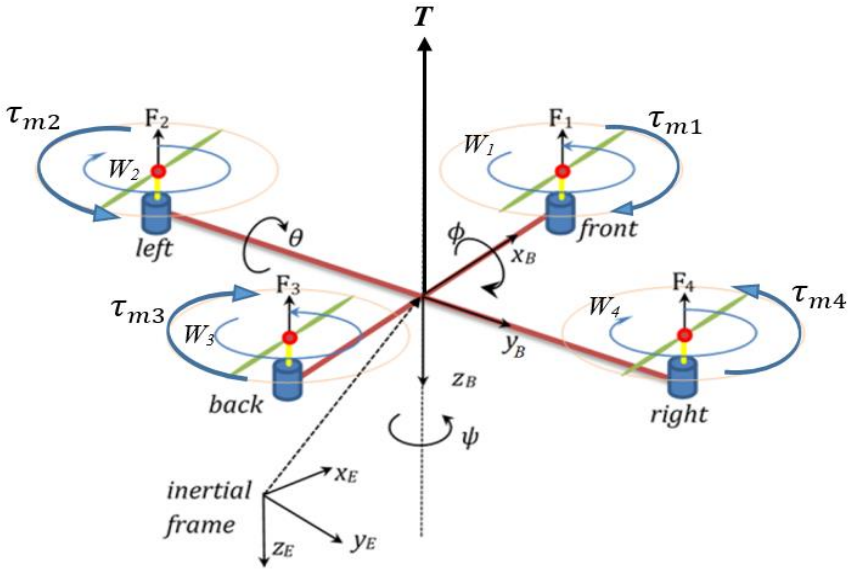

Figure 1. The inertial and body frames of the quadcopter

The quadcopter has six degrees of freedom in terms of linear position ξ = (x, y, z) and the attitude (angular position) which is defined by Euler angles H = (roll (ϕ), pitch (Θ), yaw (ψ)) with respect to the inertial frame. The Euler angles determine the rotation of the quadcopter around each axis. Roll angle ϕ determines the rotation around x-axis while Pitch angle Θ determines the rotation around y-axis and yaw angle ψ determines the rotation around z-axis. The rotation of angular velocity in the Inertial frame ($\dot{\phi}$, $\dot{\square}$, $\dot{\psi}$) to the angular velocity in the body frame (ẋ, ẏ , ż) can be obtained by

$$\boldsymbol{V} = \boldsymbol{W}_{\mathrm{H}}\dot{\boldsymbol{\Theta}} \tag{1}$$

$$\begin{bmatrix} p \\ q \\ r \end{bmatrix} = \begin{bmatrix} 1 & 0 & -s_{\square} \\ 0 & c_{\phi} & c_{\square}s_{\phi} \\ 0 & -s_{\phi} & c_{\square}s_{\phi} \end{bmatrix} \begin{bmatrix} \dot{\phi} \\ \dot{\square} \\ \dot{\psi} \end{bmatrix} \tag{2}$$

where $c_{\phi} = \cos(\phi)$, $s_{\phi} = \sin(\phi)$, $c_{\square} = \cos(\square)$, $s_{\square} = \sin(\square)$. $\boldsymbol{W}_{\mathrm{H}}$ is the transformation matrix for angular velocities from inertial frame to the body frame. $\boldsymbol{V}$ represents the angular velocity vector with respect to the body frame. $\dot{\square}$ represents the time derivative vector of the Euler angles (roll (ϕ), pitch (Θ), yaw (ψ)).

Also, the rotation matrix R can be used to transform the states from the body frame to the inertial frame. The matrix R has orthogonal property so $\boldsymbol{R}^{T} = \boldsymbol{R}^{-1}$ [1, 9-11].

$$\mathbf{R}=\begin{bmatrix} c_{\psi}c_{\square} & c_{\psi}s_{\square}s_{\phi} - s_{\psi}c_{\phi} & c_{\psi}s_{\square}c_{\phi} + s_{\psi}s_{\phi} \\ s_{\psi}c_{\square} & s_{\psi}s_{\square}s_{\phi} + c_{\psi}c_{\phi} & s_{\psi}s_{\square}c_{\phi} - c_{\psi}s_{\phi} \\ -s_{\square} & c_{\square}s_{\phi} & c_{\square}c_{\phi} \end{bmatrix} \tag{3}$$

The quadcopter has four motors which are used to provide it with the required thrust force (T) in the direction of the body z-axis.

$$T = \sum_{i=1}^{4} T_i = k(w_1^2 + w_2^2 + w_3^2 + w_4^2) \tag{4}$$

where:

$$T_i = f_i = kw_i^2$$

where T_i is the thrust force generated by i-th motor. k is the thrust factor and $w_i$is the angular velocity of the i-th motor. Also, the motors will generate torques τ_ϕ , τ_θ and τ_ψ in the direction corresponding to the body frame [10, 11].

$$\boldsymbol{\tau}_B = \begin{bmatrix} \tau_\phi \\ \tau_\theta \\ \tau_\psi \end{bmatrix} = \begin{bmatrix} lk(-w_2^2 + w_4^2) \\ lk(-w_1^2 + w_3^2) \\ k(w_2^2 + w_4^2 - w_1^2 - w_3^2) \end{bmatrix} = \begin{bmatrix} lU_2 \\ lU_3 \\ U_4 \end{bmatrix} \quad (5)$$

where l is the distance from the center of motor to the center of mass of the quadcopter. U_2 , U_3 and $U_4$are input forces to the quadcopter generated by motors.

$$U_2 = f_2 - f_4 = k(-w_2^2 + w_4^2) \quad (6)$$
$$U_3 = f_1 - f_3 = k(-w_1^2 + w_3^2 \quad (7)$$
$$U_4 = f_2 + f_4 - f_1 - f_3 = k(w_2^2 + w_4^2 - w_1^2 - w_3^2) \quad (8)$$

Also, each motor will generate torque τ_{m_i} around its rotor axis.

$$\tau_{m_i} = dw_i^2 + I_m \dot{w}_i \quad (9)$$

where d is the drag factor, $I_m$is the moment of inertia of rotor and $\dot{w}_i$ is the angular acceleration of i-th motor. Generally, $\dot{w}_i$ is very small so it can be omitted.

$$\tau_{m_i} = dw_i^2 \quad (10)$$

The Inertia matrix $\boldsymbol{I}$ of the quadcopter is diagonal with $I_{xx} = I_{yy}$ because the body of a quadcopter is assumed to be symmetrical.

$$\boldsymbol{I} = \begin{bmatrix} I_{xx} & 0 & 0 \\ 0 & I_{yy} & 0 \\ 0 & 0 & I_{zz} \end{bmatrix} \quad (11)$$

The dynamic equations (motion equations) of the quadcopter are represented by its linear acceleration $(\ddot{x}, \ddot{y}, \ddot{z})$ and angular acceleration $(\ddot{\phi}, \ddot{\theta}, \ddot{\psi})$, which can be derived by Euler-Lagrange equations of motion and previous equations (1-11).
The Lagrange $\mathcal{L}$ equation is the algebraic sum of translational E_{trans}, rotational E_{rot}, and potential E_{pot} energies. It can be defined as [10]:

$$\mathcal{L}(\boldsymbol{o}, \dot{\boldsymbol{p}}) = E_{trans} + E_{rot} + E_{pot}$$
$$= \frac{m}{2}\dot{\boldsymbol{\xi}}^T\ddot{\boldsymbol{\xi}} + \frac{1}{2}\boldsymbol{v}^T\boldsymbol{I}\boldsymbol{v} - mgz \quad (12)$$

where

$$\boldsymbol{o} = \begin{bmatrix} \boldsymbol{\xi} \\ \boldsymbol{H} \end{bmatrix} = [x, y, z, \phi, \theta, \psi\ ]^T$$

External forces and torques can be represented by the following equations:

$$\begin{bmatrix} \boldsymbol{f} \\ \boldsymbol{\tau} \end{bmatrix} = \frac{d}{dt}\left(\frac{\partial \square}{\partial \dot{o}}\right) - \frac{\partial \square}{\partial o} \tag{13}$$

Because linear and angular components are not independent, they should be studied separately. Therefore, the linear Euler-Lagrange equation are

$$\boldsymbol{f} = \boldsymbol{R}\boldsymbol{T}^{B} = m\,\ddot{\boldsymbol{\xi}} + mg\begin{bmatrix} 0 \\ 0 \\ 1 \end{bmatrix} \tag{14}$$

where T^B is the thrust force vector in the direction of body axis and equal to

$$\boldsymbol{T}^{B} = [0 \quad 0 \quad \boldsymbol{T}]^{T}$$

and therefore

$$\ddot{\boldsymbol{\xi}} = \frac{\boldsymbol{R}}{m}\begin{bmatrix} 0 \\ 0 \\ \boldsymbol{T} \end{bmatrix} - g\begin{bmatrix} 0 \\ 0 \\ 1 \end{bmatrix}$$

$$\begin{bmatrix} \ddot{x} \\ \ddot{y} \\ \ddot{z} \end{bmatrix} = \frac{T}{m}\begin{bmatrix} c_{\psi}s_{\square}c_{\phi} + s_{\psi}s_{\phi} \\ s_{\psi}s_{\square}c_{\phi} - c_{\psi}s_{\phi} \\ c_{\square}c_{\phi} \end{bmatrix} - g\begin{bmatrix} 0 \\ 0 \\ 1 \end{bmatrix}$$

$$\left.\begin{aligned} \ddot{x} &= \frac{U1}{m}(c_{\psi}s_{\square}c_{\phi} + s_{\psi}s_{\phi}) \\ \ddot{y} &= \frac{U1}{m}(s_{\psi}s_{\square}c_{\phi} - c_{\psi}s_{\phi}) \end{aligned}\right\} \qquad \ddot{z} = \frac{U1}{m}c_{\square}c_{\phi} - g \tag{15}$$

where *U1* is equal to the thrust force *T* generated by the motors. *m* represents the mass of the quadcopter.
The relations between angular velocity of motors w_i and generated forces *U1, U2, U3*, and *U4* by motors can be presented in the matrix form [9-12]

$$\begin{bmatrix} w_1^2 \\ w_2^2 \\ w_3^2 \\ w_4^2 \end{bmatrix} = \begin{bmatrix} \frac{1}{4k} & 0 & \frac{-1}{2k} & \frac{-1}{4d} \\ \frac{1}{4k} & \frac{-1}{2k} & 0 & \frac{1}{4d} \\ \frac{1}{4k} & 0 & \frac{1}{2k} & \frac{-1}{4d} \\ \frac{1}{4k} & \frac{1}{2k} & 0 & \frac{1}{4d} \end{bmatrix}\begin{bmatrix} U1 \\ U2 \\ U3 \\ U4 \end{bmatrix} \tag{16}$$

The angular Euler-Lagrange equations are

$$\boldsymbol{\tau}_B = \boldsymbol{J}\ddot{\boldsymbol{H}} + \boldsymbol{C}(\boldsymbol{H}, \dot{\boldsymbol{H}})\dot{\boldsymbol{H}} \tag{17}$$

where *J* is the Jacobian matrix transform from V to $\dot{H}$ as

$$\boldsymbol{J} = \boldsymbol{W}_H^T \boldsymbol{I} \boldsymbol{W}_H$$

$$\boldsymbol{J} = \begin{bmatrix} I_{xx} & 0 & -I_{xx}s_\theta \\ 0 & I_{yy}c_\phi^2 + I_{zz}s_\phi^2 & (I_{yy} - I_{zz})c_\phi s_\phi c_\theta \\ -I_{xx}s_\theta & (I_{yy} - I_{zz})c_\phi s_\phi c_\theta & I_{xx}s_\theta^2 + I_{yy}s_\phi^2 c_\theta^2 + I_{zz}c_\phi^2 c_\theta^2 \end{bmatrix} \quad (18)$$

C matrix is the Coriolis term containing the gyroscope and centripetal terms [10].
Now, angular acceleration equations of the quadcopter can be derived from equation (17) as

$$\ddot{\boldsymbol{H}} = \boldsymbol{J}^{-1}(\boldsymbol{\tau}_B - \boldsymbol{C}(\boldsymbol{H}, \dot{\boldsymbol{H}})\dot{\boldsymbol{H}}) \quad (19)$$

By compensating the value of **H** in equation (19), the following angular acceleration equations can be found as

$$\left.\begin{aligned} \ddot{\phi} &= \frac{I_y - I_z}{I_x}\dot{\theta}\dot{\psi} - \frac{J_r}{I_x}W_r\dot{\theta} + \frac{U_2}{I_x} \\ \ddot{\theta} &= \frac{I_z - I_x}{I_y}\dot{\phi}\dot{\psi} - \frac{J_r}{I_y}W_r\dot{\phi} + \frac{U_3}{I_y} \\ \ddot{\psi} &= \frac{I_x - I_y}{I_z}\dot{\theta}\dot{\phi} + \frac{U_4}{I_z} \end{aligned}\right\} \quad (20)$$

where W_r is the algebraic sum of the angular speed of motors.

$$W_r = -w_1 + w_2 - w_3 + w_4$$

J_r is the inertia of the motor and it is a very small value and often can be omitted so, the equation (20) will instead become:

$$\left.\begin{aligned} \ddot{\phi} &= \frac{I_y - I_z}{I_x}\dot{\theta}\dot{\psi} + \frac{U_2}{I_x} \\ \ddot{\theta} &= \frac{I_z - I_x}{I_y}\dot{\phi}\dot{\psi} + \frac{U_3}{I_y} \\ \ddot{\psi} &= \frac{I_x - I_y}{I_z}\dot{\theta}\dot{\phi} + \frac{U_4}{I_z} \end{aligned}\right\} \quad (21)$$

Equations (15) and (21) represent linear and angular motions of the quadcopter respectively. For researchers to achieve better quadcopter performance, this mathematical modeling affords us the ability to simulate and test multiple different scenarios in Matlab/Simulink or a similar environment [9-12].
Linear and angular velocity states can be calculated by integration of the equations (15) and (21). Also, linear and angular position states can be calculated by double integrating the equations (15) and (21) respectively. These 12 states $(x, \dot{x}, y, \dot{y}, z, \dot{z}, \phi, \dot{\phi}, \theta, \dot{\theta}, \psi, \dot{\psi})$ represent the measured states by the sensors connected to the controller of the quadcopter.

3. The Proposed Control Model

Quadcopters used for delivery applications almost exclusively avail of the autonomous flight technique. GPS signal is used to continuously measure the linear position of the quadcopter, to retain control of it, and ultimately drive it to follow the desired path and arrive at it destination. However, as detailed in Section 1, there is a critical challenge to the success of this application method. Interference from some environmental stimuli can cause the GPS signal to be denied. The previous methods used to solve the problem of GPS signal denial are special methods for certain applications and short distances as mentioned in section 1[2, 4-6].

To solve this undesirable consequence of GPS signal denial, we propose a new, multimode control algorithm to make quadcopter work properly in most environments. The algorithm, presented in Figure 2, is distinctive from previous work, due to alternating control modes plus an appropriate filter to improve error rates.

First, the controller would function in one of two alternating control modes; GPS control mode and accelerometer control mode. Once a GPS signal denial is detected, it triggers a shift from one control mode to the other. Specifically, when the quadcopter's GPS signal is denied during GPS control mode, accelerometer control mode will be activated and will begin to measure the linear position of the quadcopter from the accelerometer sensor signal.

The first key of our proposed algorithm is to use multimode control algorithm (GPS and Accelerometer control modes). GPS control mode is given higher priority than the accelerometer control mode because it provides more accurate information [6]. The mode selector is tested continuously the number of satellites connected to the GPS sensor. It will change the control mode when the number of satellites associated with the GPS sensor becomes less than four.

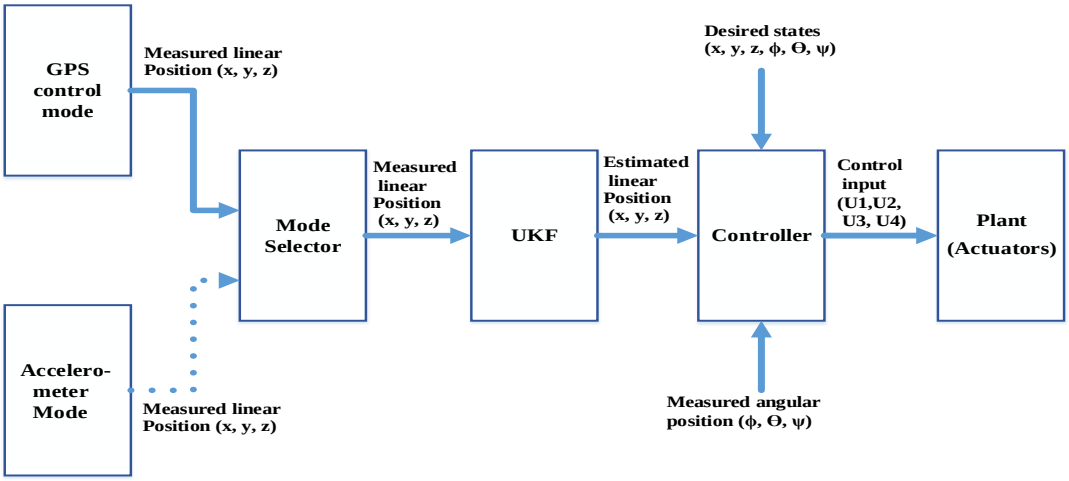

Figure 2. Our proposed model

The second key feature of this new algorithm addresses noise signals caused by physical sensors. Since both GPS and accelerometer sensors exhibit errors caused by the noise signals, UKF is inserted to the control algorithm with the goals to a) decrease the effect of these errors (in the measured states of sensors), and b) provide more accurate states to the controller, and c) increase the reliability of the overall control algorithm and optimize performance of the quadcopter. The proposed algorithm shown, in Figure 2, has less complexity than the algorithms that continuously merge GPS and accelerometer sensors. The latter needs more complicated calculation and it would consume more power than the shifting multimode algorithm we present in this paper, which has the benefit of being more resource-efficient.

4. PID Controller

Control of the attitude and position of the quadcopter is implemented by applying appropriate thrust (T) and torques (τ_B) which are achieved by angular velocities of rotors (w_1, w_2, w_3 *and* w_4). Appropriate thrust and torques can be determined using the traditional PID-feedback controller like methods in [1, 2, 8-11, 15]:

$$PID(e) = k_p e(t) + k_I \int_0^t e(\tau)d\tau + k_D \frac{d}{dt} state \qquad (22)$$

where

$$e(t) = \text{desired state(t)} - \text{measured state(t)}$$

k_p, k_I and k_D are the proportional, integral and derivative gains respectively.

However, the traditional PID controller may cause a problem. Namely, if the desired input takes a step function, then the output of the derivative will be an impulse signal which could bring the motors to the state of saturation and push the system outside the controlled space. To avoid this problem, we included a modified PID controller (hereafter referred to as PI-D). Figure 3 shows the structure of the PI-D controller, where the error signal is an input signal to the proportional and integral line while the derivative term is calculated directly from sensor data [15].

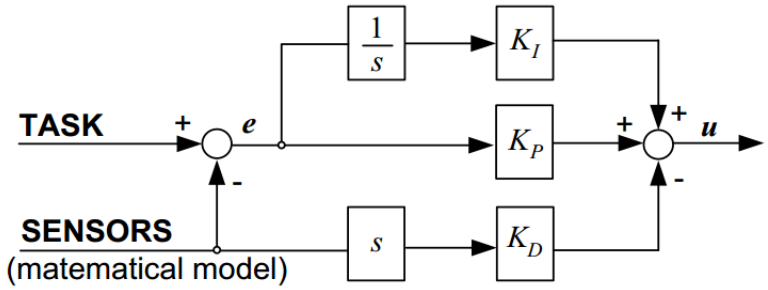

Figure 3. Modified PID (PI-D) controller structure

The use of PI-D Controller avoids the control system from error signal (e) problem if it is step input where the derivative of this type of signal is impulse signal. Therefore, the impulse signal maybe causes saturation in controller and push the system to unstable situation.

4.1 Altitude PI-D Control

The required appropriate thrust force, U1, can be calculated by:

$$U1 = k_{p_z} e_z + k_{I_z} \int e_z - k_{D_z} \dot{z}_{meas} + mg \tag{23}$$

where k_{p_z},k_{I_z} and k_{D_z} are altitude PI-D gains controller; e_z is the altitude error $e_z = z_{des} - z_{meas}$, where z_{meas} and z_{des} are desired and measured altitude respectively; g is the earth's gravity.

4.2 Attitude PI-D Control

Three control signals (presented within equation (21)) are used to achieve the required quadcopter attitude. These signals are used to control the Roll (ϕ), Pitch (Θ) and Yaw (ψ) angles which describe the warp angles of the quadcopter's body around x-axis, y-axis and z-axis respectively. The control signals can be calculated by the following equations [15]:

4.2.1 Roll Control

The torque U2 to rotate the quadcopter around the x-axis can be calculated by:

$$U2 = k_{p_\phi} e_\phi + k_{I_\phi} \int e_\phi - k_{D_\phi} \dot{\phi}_{meas} \tag{24}$$

where k_{p_ϕ},k_{I_ϕ} and k_{D_ϕ} are roll angle PI-D gains controller; e_ϕ is roll angle error $e_\phi = \phi_{des} - \phi_{meas}$, where ϕ_{des} and ϕ_{meas} are desired and measured roll angle respectively.

4.2.2 Pitch Control

The torque U3 to rotate the quadcopter around the y-axis can be calculated by:

$$U3 = k_{p_\theta} e_\theta + k_{I_\theta} \int e_\theta - k_{D_\theta} \dot{\theta}_{meas} \tag{25}$$

where k_{p_θ},k_{I_θ} and k_{D_θ} are pitch angle PI-D gains controller; e_θ is pitch angle error $e_\theta = \theta_{des} - \theta_{meas}$, where θ_{des} and θ_{meas} are desired and measured pitch angle respectively.

4.2.3 Yaw Control

The torque U4 to rotate the quadcopter around the z-axis can be calculated by:

$$U4 = k_{p_\psi} e_\psi + k_{I_\psi} \int e_\psi - k_{D_\psi} \dot{\psi}_{meas} \quad (26)$$

where k_{p_ψ},k_{I_ψ} and k_{D_ψ} are yaw angle PI-D gains controller; e_ψ is yaw angle error $e_\psi = \psi_{des} - \psi_{meas}$, where ψ_{des} and ψ_{meas} are desired and measured yaw angle respectively.

The quadcopter has 6 DOF and only 4 actuators (motors) so it is not possible to control all these DOF directly. The control equations (23) to (26) are used to directly control 4 DOF (z, ϕ, □, ψ). The roll and pitch angles make the quadcopter move towards the desired x and y. So, the desired x and y will be used first to calculate the desired roll and pitch angles to be able to control x and y positions indirectly. The equations which are used to calculate desired roll and pitch angles are frequently written in terms of desired x and y accelerations. The following equations are used to calculate desired acceleration though desired x, y and z [1]:

$$\ddot{x}_{des} = (k_{p_x} e_x + k_{I_x} \int e_x - k_{D_x} \dot{x}_{meas})/m \quad (27)$$

$$\ddot{y}_{des} = (k_{p_y} e_y + k_{I_y} \int e_y - k_{D_y} \dot{y}_{meas})/m \quad (28)$$

$$\ddot{z}_{des} = (k_{p_z} e_z + k_{I_z} \int e_z - k_{D_z} \dot{z}_{meas} - mg)/m \quad (29)$$

The equations below represent the relations between desired linear accelerations with respect to the inertial frame, and the desired related angles roll, pitch and yaw with respect to the body frame [1]:

$$\phi_{des} = sin^{-1}\left(\frac{\ddot{x}_{des} s_\psi - \ddot{y}_{des} c_\psi}{\sqrt{\ddot{x}_{des}^2 + \ddot{y}_{des}^2 + (\ddot{z}_{des} + g)^2}}\right) \quad (30)$$

$$□_{des} = tan^{-1}\left(\frac{\ddot{x}_{des} c_\psi - \ddot{y}_{des} s_\psi}{\ddot{z}_{des} + g}\right) \quad (31)$$

The block diagram of the quadcopter with a PI-D controller is as shown in Figure 4 [1].

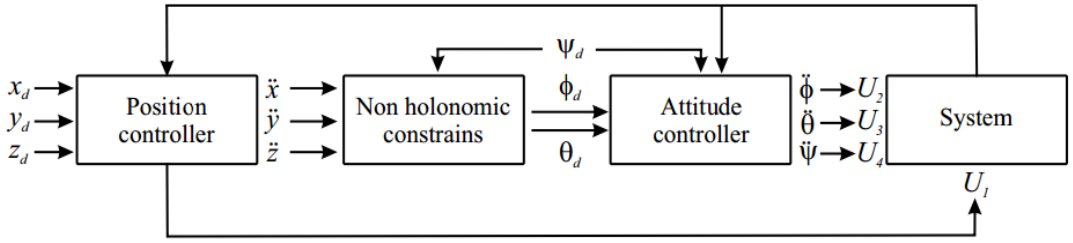

Figure 4. Block diagram of the control algorithm of quadcopter with PI-D controller

5. Unscented Kalman Filter (UKF)

For a control system to work effectively, the state estimation is a critical task, and it relies heavily on the degree of noise and uncertainties. In real time control of the quadcopter, unknown results in the measurement of states can occur due to the measurement algorithms or uncertainties of the physical device or both. For instance, the gyroscope, accelerometer and GPS sensors are used to control the quadcopter, and they lead to a signal with noise. Often, the noise caused by sensors leads to unknown results that subsequently drives the system to non-optimal or unstable states. For this reason, different algorithms have been proposed to decrease, or ideally eliminate, the undesirable effects of noise on the control algorithm.

The Unscented Kalman Filter (UKF) is a modern nonlinear filter used to estimate the optimal states of nonlinear systems corrupted by Gaussian noise [15-18]. UKF is an efficient method to calculate the statistics of a random variable by a nonlinear transformation called *Unscented transformation (UT)*. UKF is based on a simple assumption that it is easier to approximate a Gaussian distribution than to approximate an arbitrary nonlinear function or transformation. When the UKF is applied to the data, it generates a finite number of points, called *sigma points*, to sample the prior distribution, and keeps the sample mean and sample covariance the same as the original distribution [16], [17].
It has two phases: *the time-update (prediction phase)* and *the measurement-update (correction phase)*. In the prediction phase, sigma points are achieved for the last available estimated states and each point is assigned a weight. Thereafter, the sigma points are put through the nonlinear model equations to then obtain predicted states. In the measurements-update phase, the predicted states are corrected by adding the effect of the information obtained from the new state measurements to estimate the actual states [16], [18].
UKF predicts the states of the last estimated states by the following equation:

$$\widetilde{\boldsymbol{X}}_{k+1|k} = \boldsymbol{\phi}_{k+1|k}\left[\boldsymbol{X}_{k|k}\right] + \boldsymbol{G}_k \tag{32}$$

The discrete predicted states $\widetilde{\boldsymbol{X}}_{k+1|k}$ at k+1 are updated with the measurement information by the following equation:

$$\widehat{\boldsymbol{X}}_{k+1|k} = \mathbf{H}_{k+1|k}\left[\widetilde{\boldsymbol{X}}_{k+1|k}\right] + \boldsymbol{V}_{k+1} \tag{33}$$

where $\boldsymbol{\phi}_{k+1|k}$ is the discrete state transition matrix from k to k+1,$\boldsymbol{X}_{k|k}$ is estimated states at k,$\boldsymbol{G}_k$ is the process noise vector at k, $\widehat{\boldsymbol{X}}_{k+1}$ is the estimated state vector at k+1, $\boldsymbol{V}_{k+1}$ is the measurement noise vector, $\mathbf{H}_{k+1|k}$ is the observation matrix. The state transition matrix is linear and derived from dynamic model acceleration equations of the quadcopter. Only the observation matrix $\mathbf{H}_{k+1|k}$ contains nonlinear equations and it is calculated by the following equation:

$$\mathbf{H}_{k+1|k} = \sum_{i=0}^{2*n} W_i * \boldsymbol{H}(X_{i,\ k+1|k}^{\tilde{x}}) + X_{i,\ k+1}^{V} \tag{34}$$

where W_i are the weights, $X_{i,\ k+1|k}^{\tilde{x}}$ are the sigma points which describe the predicted states $\tilde{X}_{k+1|k}$, $X_{i,\ k+1}^{V}$ are the sigma points describing the measurement noise [16-20].
The number of sigma points depends on the dimensionality of the system. The general formula to calculate the number of sigma points is 2n+1, where n is the dimension of the system.
The following equations are used to calculate the sigma points for the predicted states$\tilde{X}_{k+1|k}$ [16], [18]:

$$X_0 = \overline{\tilde{X}}$$
$$X_i = \overline{\tilde{X}} + (\sqrt{(n+\lambda)p_{\tilde{x}\tilde{x}}})_i \qquad \text{i=1, ……., n}$$
$$X_{i+n} = \overline{\tilde{X}} + (\sqrt{(n+\lambda)\boldsymbol{p}_{\tilde{x}\tilde{x}}})_i \qquad \text{i=n+1, ……., 2n}$$

where $\overline{\tilde{X}}$ is the mean of the predicted states $\tilde{X}_{k+1|k}$, N is the dimension of the predicted states, λ is the scaling factor which tells how far from the mean we should choose our sigma points, $\boldsymbol{p}_{\tilde{x}\tilde{x}}$ is the covariance matrix of predicted states, $(\sqrt{(n+\lambda)\boldsymbol{p}_{\tilde{x}\tilde{x}}})_i$ is the i-th column of the square root weighted covariance [16].

6. Simulation Setup

Simulink was used to generate the simulation of the quadcopter's attitude and trajectory control. Figure 5 shows the block diagram which is used to perform all controller modes. UKF is added to the control system as a state's estimator, in order to remove or decrease the effect of noise on the states. Sensor noise is induced in different places of the simulation to make it more realistic.

6.1 GPS mode control

In this mode, GPS sensor is used to provide the controller with real time linear positions (x, y, z) of quadcopter depending on the signals received from multi satellites. Linear and angular positions, calculated by equations (15) and (21) respectively, represent the information provided by ideal sensors but in the real world there is no ideal sensor so a Gaussian noise is added to the information obtained by motion equations. Figure 5 shows the Simulink block diagram of GPS mode.

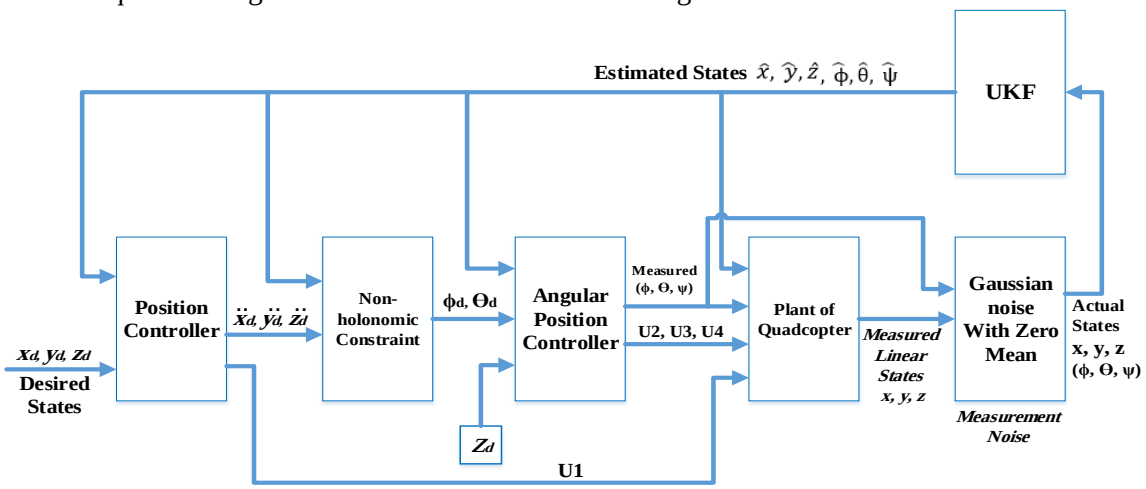

Figure 5. Simulink block diagram of GPS control mode with the UKF

6.2 Multimode Control

Accelerometer sensor is a microelectromechanical device used to provide position information for the body directly connected to it. Unfortunately, this information is less accurate compared to the information provided by GPS sensor because it is heavily influenced by vibration in the body of quadcopter, and thus results in inaccurate data. As mentioned previously, accelerometer signal will be used as an alternative to GPS signal. Accelerometer control mode will keep the quadcopter under control with less performance. Figure 6 shows the Simulink block diagram of the multimode controller.

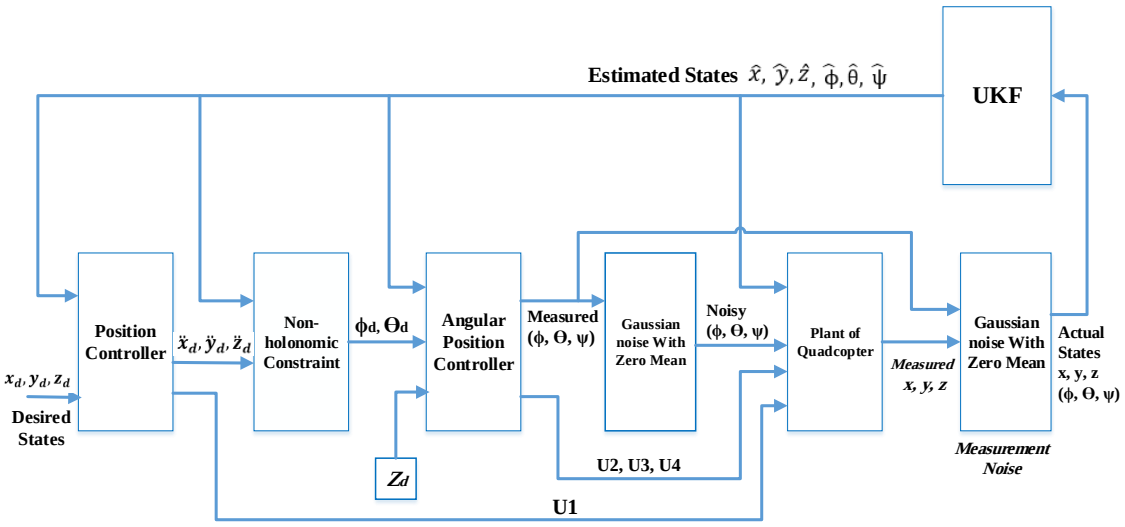

Figure 6. Simulink block diagram of multimode (GPS + Accelerometer) control mode with UKF

Gaussian noise is added to the calculated attitude values to represent the accelerometer signal because attitude values directly influence the linear position equations (15) [21].
As we mentioned earlier, the estimation filter (UKF) is used with all control modes to improve the performance of quadcopter through flight.

7. Results and Discussions

The quadcopter model was simulated and tested to follow the desired trajectory under different control modes (GPS mode, accelerometer mode and multimode). The actual responses under different modes were obtained by using a modified PI-D controller with a UKF. The mathematical equations which are used to test the proposed control algorithm in this paper are: The quadcopter dynamic equations (15), (21), the PI-D control equations (23-26), the desired angles (Roll, Pitch) and linear accelerations equations (27-31) as well as the available UKF Matlab block. All tests are performed using block diagrams in figures (5, 6). The value of parameters needed to perform the Simulink can be shown in Table 1. The system was simulated in Matlab version R2018a.

Table 1: Parameters values of the quadcopter for simulations

Parameter	Value	Parameter	Value	Parameter	Value
m	0.8 kg	$K_{p\psi}$	0.21	K_{py}	2
g	9.81 m/s^2	K_{dx}	2.8	K_{pz}	10
l_{xx}	0.015 kg.m^2	K_{dy}	2.8	$K_{p\phi}$	1.5
l_{yy}	0.015 kg.m^2	K_{dz}	7	$K_{p\Theta}$	1.5
l_{zz}	0.02 kg.m^2	$K_{d\phi}$	0.5	K_{Iy}	0.0088
k	3.13*10^{-5}	$K_{d\Theta}$	0.5	K_{Iz}	2
d	7.5*10^{-7}	$K_{d\psi}$	0.7997	$K_{I\phi}$	0.8775
l	0.25 m	K_{Ix}	0.0088	$K_{I\Theta}$	0.8775
		K_{px}	2	$K_{I\psi}$	0.0123

7.1 Result of GPS Control Mode

This mode is implemented with Simulink blocks diagram shown in Figure 5. Actual measured states (which represent the GPS signal) are used by the PI-D controller to control the quadcopter and make it follow the desired trajectory. Figure 7 shows the response of the quadcopter with very small steady state error less than one meter. In this mode, no problem with GPS signal is assumed.

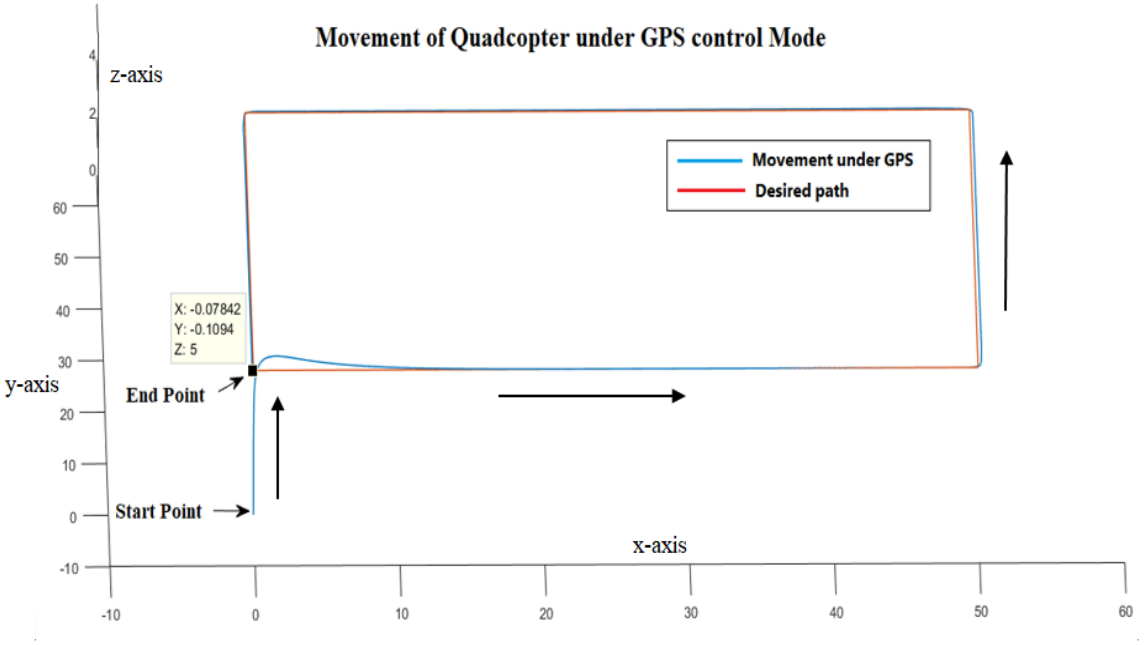

Figure 7. Response of quadcopter under GPS mode control

At first, the quadcopter takes off for desired altitude (z). Then it follows desired trajectory in x-y plane for 200 seconds and back again to the start point.

7.2 Result of GPS + Accelerometer Control Mode

Firstly, we should test the behaviour of the quadcopter when GPS signal is denied for the reasons mentioned earlier. Figure 8 shows a comparison between the desired path and the actual path of a quadcopter if 5 seconds of GPS signal is denied at the 70th second of simulation time.

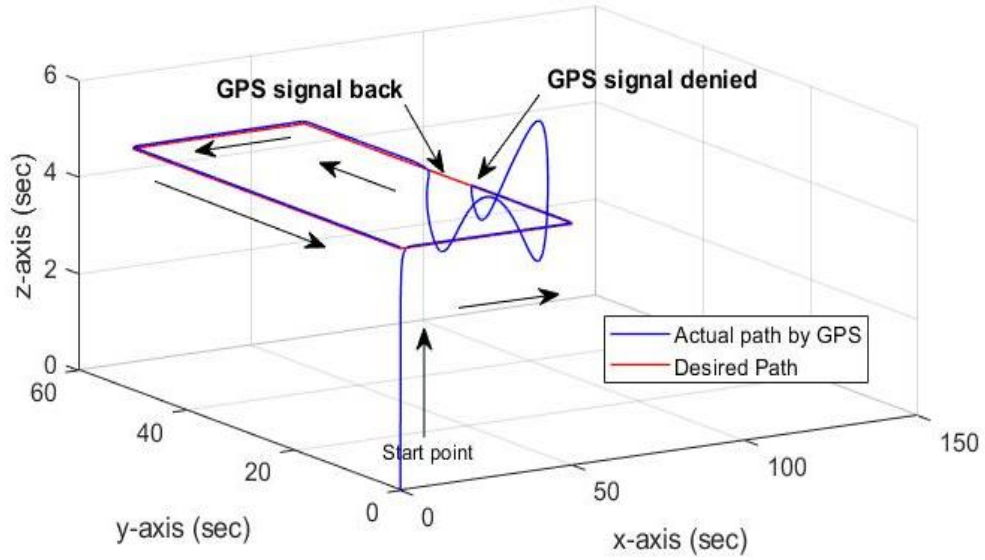

Figure 8. Response of quadcopter under GPS mode with GPS denied signal problem.

We can observe that, during the GPS disconnection, the quadcopter will be out of control and move randomly because the measured position by GPS sensor become about zero and the quadcopter seems

very far from the desired position. Therefore, the input error signal to the controller become large and that is lead the controller try to push the quadcopter strongly to follow the desired path. But in fact, the controller made the quadcopter move very strongly in a very far direction from the desired path. We can also observe that the probability of quadcopter damage is very large during the period of GPS signal denial without found alternative signal to it.

To solve the GPS problem, the system switches from the GPS control mode to the accelerometer control mode. Under this alternative mode, the accelerometer sensor provides the controller with linear position data of the quadcopter.

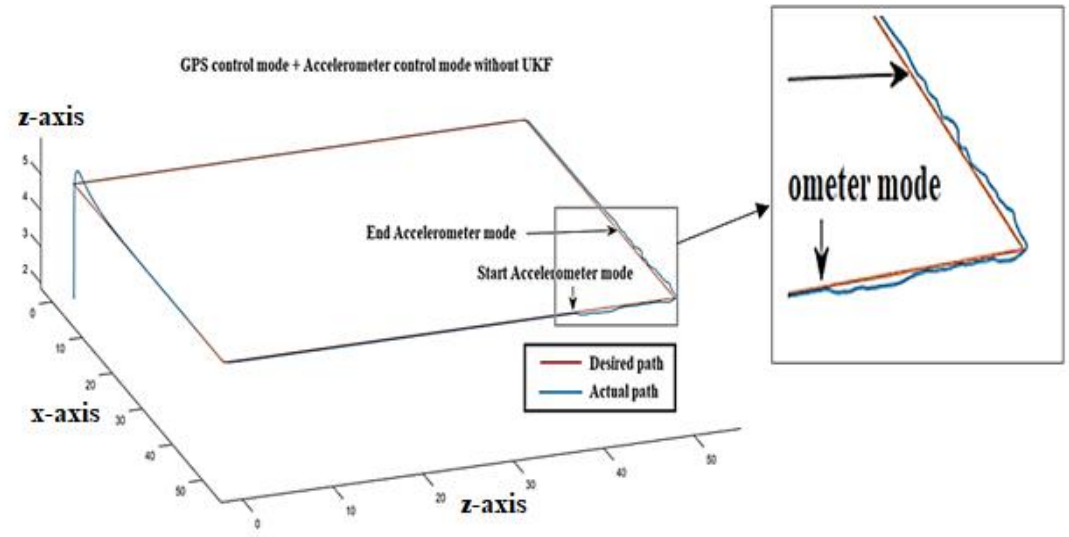

(a)

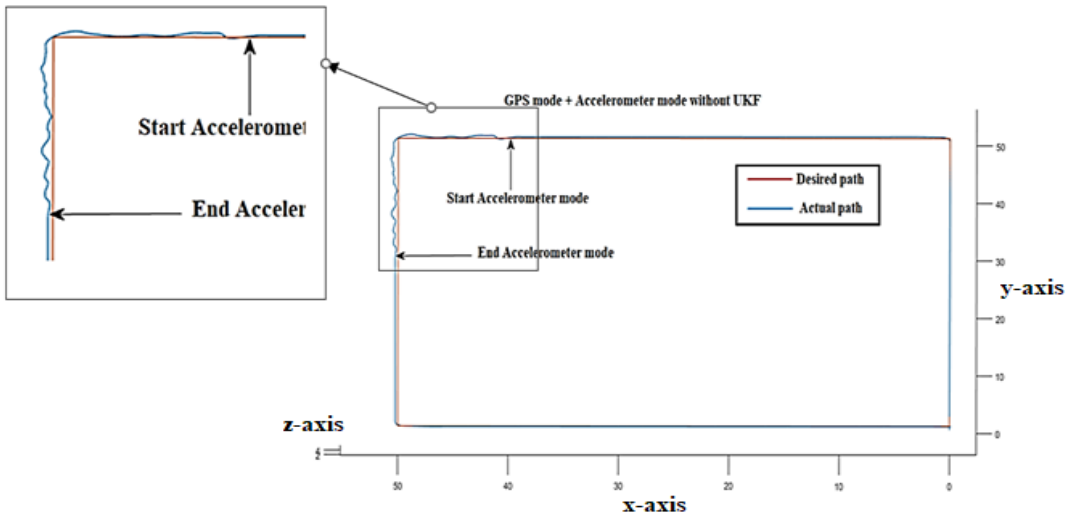

(b)

Figure 9. GPS control mode with accelerometer control mode as a solution for GPS signal denied. Figures **9a** and **9b** represent side and top view of the quadcopter response.

As we mentioned earlier, information provided by an accelerometer sensor is less accurate than information provided by GPS sensor. However, during a finite period of GPS signal denial, the

derived position information by accelerometer sensor is sufficient enough for the quadcopter to remain under control and to follow the desired path with more modest fluctuations, as shown in Figures 9a, b. We can compare the actual path here (Figure 9.), to the actual path in a simulation with only GPS information, and no alternative control mode (Figure 8.).

7.3 Result of Multimode control with UKF

All simulations previously performed without using UKF. With the addition of this filter, we aimed to reduce the size of error (noise) for sensor measurements. Figure 10 represents two actual-path simulations of 30 seconds of the quadcopter under accelerator control mode - one simulation has the UKF applied (green line), and one shows the path without the UKF applied (blue line). We observed that the impact of the UKF appears clearly when there is a fluctuation in the movement of the quadcopter. The filter improved controller performance and reduced fluctuation in the quadcopter's motion, as shown in Figure 10a, b, c.

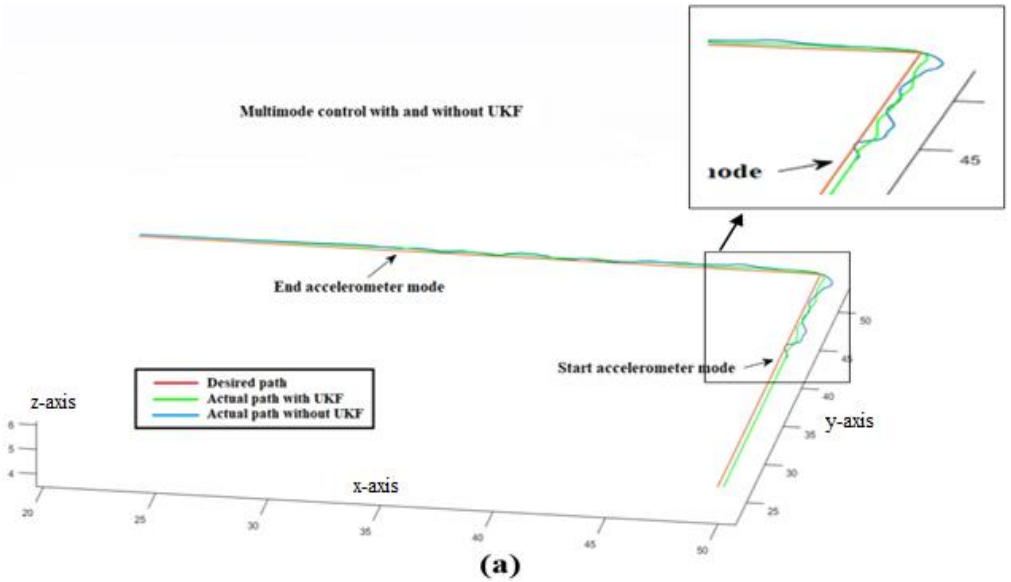

(a)

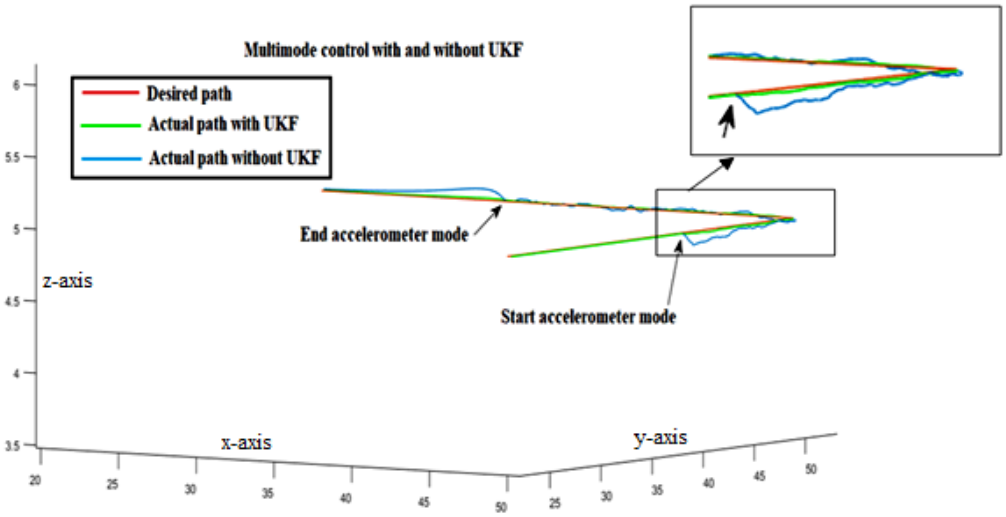

(b)

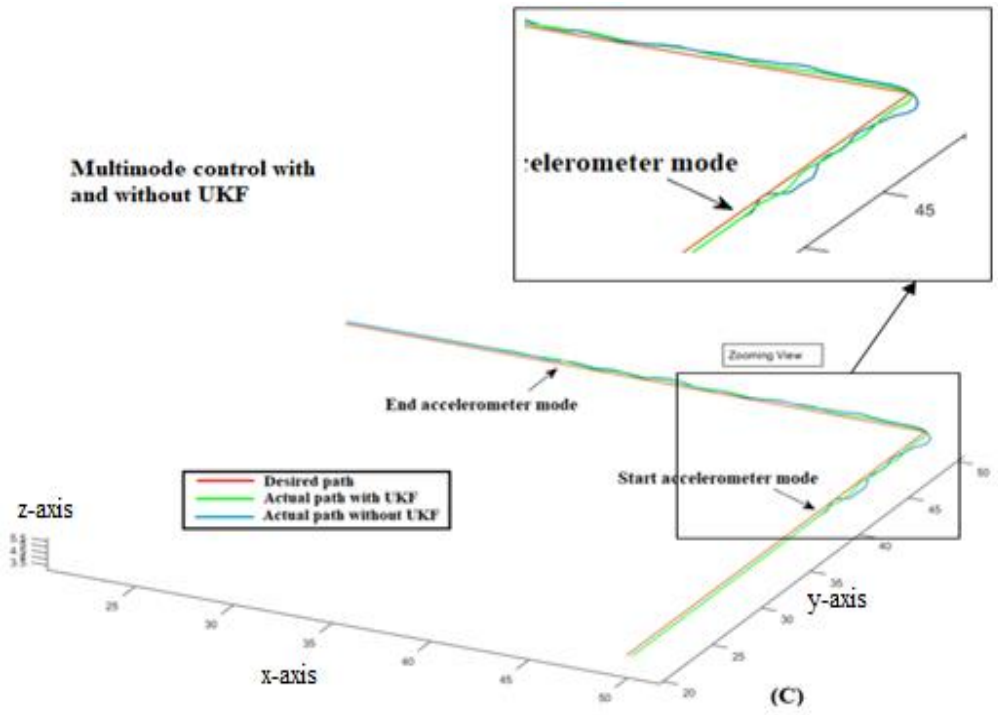

Figure 10. Different angles of view for the response of quadcopter under Multimode control with and without UKF

It is very clear from Figure 10 that UKF decreases the fluctuation of quadcopter response especially in the accelerometer control mode and it tries to keep the response close to the desired path. Important comparison is made in table 2to show differences between our proposed algorithm and proposed algorithms in [2, 4, and 5] for three significant parameters: Suitable environments, Operation distance, Applications. The first and second method can operate in limited environments because some environmentsveilthe connection between the quadcopter and the ground station like mountains area and this lead to make quadcopter out of control. which feed it with information that keeps it under control. Also, the RF and GSM network signals have limited operation distance and this make the first and second algorithms have limited operation distance. The third algorithm designed to operate within 50 meters while our proposed algorithm has very large operation distance. Only the third algorithm is for special application while the other are suitable for various applications.

Table 2. Comparison between our proposed algorithm and proposed algorithms in [2, 4, and 5] for three significant parameters

Parameters	Use RF round station [2]	Use GPS with Google Map [4]	Use two search lights [5]	Proposed algorithm
Environments	Limited	Limited	Limited	Most
Delivery Distance	Limited	Limited	Short	Large
Applications	various	various	Special	various

8. Conclusion

In this paper, the problem of GPS signal denial addressed during autonomous attitude and position control. A dynamic model of the quadcopter with 6- DOF has been used in our simulation. Simulation study using Simulink 2018a has been presented to show the problem of GPS signal denied through GPS control mode and its solution by accelerometer signal through accelerometer control mode. This solution is suitable for different applications environments and can be used in most autonomous flight applications of quadcopter like delivery, monitoring, agricultural and so on. While most of previous solutions are dedicated to specific applications. The results obtained in this paper show that accelerometer control mode is a reliable solution for GPS signal denied and it keeps quadcopter under control with simple fluctuations. The results show that UKF improves the controller performance and decreases the fluctuations in motion especially in the accelerometer control mode and make control of quadcopter more reliable.

References

[1] Camarillo-Gómez, K.A., Pérez-Soto, G.I. and Rodríguez-Reséndiz, J., 2018. "Comparison of PD, PID and Sliding-Mode Position Controllers for V–Tail Quadcopter Stability." *IEEE Access*, *vol. 6*, pp.38086-38096.

[2] Ononiwu, G., Onojo, O., Ozioko, O. and Nosiri, O., 2016. "Quadcopter Design for Payload Delivery." *J. of Comp. and Commun.*, *vol. 4*, no. 10, pp.1-12.

[3] San, K.T., Mun, S.J., Choe, Y.H. and Chang, Y.S., 2018. "UAV delivery monitoring system." In *MATEC Web of Conf.,* vol. 151, p. 04011.

[4] Haque, M.R., Muhammad, M., Swarnaker, D. and Arifuzzaman, M., 2014. "Autonomous quadcopter for product home delivery." In *2014 Int. Conf. on Electrical Eng. and Info. & Commun. Tech.*, pp. 1-5.

[5] Toda, H. and Fujiuti, K., 2018, "50 m-range distance and position measurement method by using two searchlights for autonomous flight device." *Int. J. of Eng. Research and Sci.*, *vol. 4, no.* 7.

[6] Theys, B., Notteboom, C., Hochstenbach, M. and De Schutter, J., 2015. "Design and control of an unmanned aerial vehicle for autonomous parcel delivery with transition from vertical take-off to forward flight." *Int. J. of Micro Air Vehicles*, vol. *7, no.* 4, pp.395-405.

[7] Ryu, J.H., Gankhuyag, G. and Chong, K.T., 2016. "Navigation system heading and position accuracy improvement through GPS and INS data fusion", *J. of Sensors*.

[8] Fernando, H.C.T.E., De Silva, A.T.A., De Zoysa, M.D.C., Dilshan, K.A.D.C. and Munasinghe, S.R., 2013, December. Modelling, simulation and implementation of a quadrotor UAV. In *2013 IEEE 8th Int. Conf. on Ind. and Info. Sys.*, pp. 207-212.

[9] Armah S, Yi S, Choi W and Shin D, 2016" Feedback Control of Quad-Rotors with a Matlab-Based Simulator". *American J. of App. Sci.*

[10] Alaiwi Y and Mutlu A, 2018" Modelling, Simulation and Implementation of Autonomous Unmanned Quadrotor". *J. of Machines, Tech., Materials*.

[11] Kamel, B., Yasmina, B., Laredj, B., Benaoumeur, I. and Zoubir, A.F., 2017, August. "Dynamic modeling, simulation and PID controller of unmanned aerial vehicle UAV." In *2017 7th Int. Conf. on Innovative Comp. Tech. (INTECH)*, pp. 64-69.

[12] Herrera, M., Chamorro, W., Gómez, A.P. and Camacho, O., 2015, July. "Sliding mode control: An approach to control a quadrotor." In *2015 Asia-Pacific Conf. on Comp. Aided Sys. Eng.,* pp. 314-319.

[13] Faizan Shahid, Muhammad Bilal Kadri, Nasir Aziz Jumani, Zaid Pirwani, 2016" Dynamical Modeling and Control of Quadrotor". *J. of Trans. on Machine Design*, vol. 4, no. 2.

[14] Beard, R.W., 2008. "Quadrotor dynamics and control." *Brigham Young Uni.*, *vol. 19*, no. 3, pp.46-56.

[15] Kotarski, D., Benić, Z. and Krznar, M., 2016. "Control design for unmanned aerial vehicles with four rotors." *Interdisciplinary Description of Complex Sys.: INDECS*, *vol. 14*, no. 2, pp.236-245.

[16] Fiorenzani, T., Manes, C., Oriolo, G. and Peliti, P., 2008. "Comparative study of unscented Kalman filter and extended Kalman filter for position/attitude estimation in unmanned aerial vehicles." *Institute for Sys. Analysis and Comp. Sci. (IASI-CNR), Rome, Italy, Report*, (08-08).

[17] St-Pierre, M. and Gingras, D., 2004, June. "Comparison between the unscented Kalman filter and the extended Kalman filter for the position estimation module of an integrated navigation information system." In *IEEE Intelligent Vehicles Sympo., 2004* (pp. 831-835). IEEE.

[18] Singh H, 2018 "The Unscented Kalman Filter: Anything EKF can do I can do it better". Online article accessed on April 2018. https://towardsdatascience.com/the-unscented-kalman-filter-anything-ekf-can-do-i-can-do-it-better-ce7c773cf88d

[19] Kaba, A., Ermeydan, A. and Kiyak, E., 2017, April. "Model derivation, attitude control and Kalman filter estimation of a quadcopter." In *2017 4th Int. Conf. on Electrical and Elect. Eng. (ICEEE)*, pp. 210-214.

[20] Terejanu, G.A., 2011. "Unscented Kalman filter tutorial." *Uni. of Buffalo, Buffalo*.

[21] Ferry, N., 2017. "Quadcopter Plant Model and Control System Development with MATLAB/Simulink Implementation.", *Master Thesis, Rochester Institute of Technology*. Rochester, NEW YORK.